Drainage-induced control of avalanches in foam coalescence

Alesya Mikhailovskaya, Cécile Monteux

Drainage-induced control of avalanches in foam coalescence

Alesya Mikhailovskaya[1] and Cécile Monteux[1,2*]
[1] Sciences et Ingénierie de la Matiére Molle, ESPCI Paris, PSL Research University, CNRS, Sorbonne Universités, UPMC Univ Paris 06, 75005 Paris, France and
[2] Global Station for Soft Matter, Global Institution for Collaborative Research and Education, Hokkaido University, Sapporo, Japan.
(Dated: July 13, 2020)

Surfactant foams are particularly unstable because of avalanches of coalescence which lead to an instant collapse of considerable part of the foam volume when the liquid fraction falls below a critical value. In many applications it is crucial to control the occurrence of these avalanches phenomena. By comparing the evolution of a foam made from a surfactant solution with a foam stabilized by a surface-active polymer which present different rates of drainage, we demonstrate that the occurrence of avalanches is controlled by the liquid fraction profile in the foams. Furthermore, forcing a drainage flow from the top of the foam during the foaming process provides another mean to control the liquid fraction profile in the foams and the occurence of avalanches. As a result we are able to induce or suppress avalanches in both the surfactant and the polymer foams by varying the foaming process. Finally we show that the velocity of the coalescence front is determined by the foam liquid fraction profile. Our study therefore illustrates the strong coupling between drainage and coalescence and provides means to control it by varying the type of foam stabilizer used and the foaming process.

INTRODUCTION

Liquid foams are concentrated dispersions of gas bubbles in a solution containing surface active agents required to stabilize the liquid-gas interfaces. The liquid fraction $\phi = V_{liquid}/V_{foam}$ in foams is usually small, so that the bubbles get in contact and deform into a polyhedral shape to achieve a dense structure. In this packing, bubbles are separated by thin liquid films that meet each other in liquid channels, so called Plateau borders (PBs), that are in turn connected in nodes. Such interconnected soft structure of liquid films and channels has a very high surface-to-volume ratio which makes foams indispensable in many industrial processes and in personal life products [1, 2].

Foams are thermodynamically unstable and tend to disappear because of three main destabilization mechanisms [3]. *Coarsening* occurs because of the gas diffusion from smaller bubbles to bigger ones due to the difference in Laplace pressure. *Drainage*, due to gravity, leads to very thin films which are more likely to rupture, leading to *coalescence* of bubbles. These mechanisms are strongly interrelated and foam structure is evolving under their action in a continuous manner. As an example, the coupling between drainage and coarsening has been largely explored in the literature [4–7]. As foams drains, the thickness of thin liquid films decreases while their surface area gets larger leading to coarsening acceleration. Moreover the increase in bubble size due to coarsening results in an acceleration of the drainage flow. In comparison, the coupling between drainage and coalescence has been less studied [8, 9]. Several types of coalescence scenarios can occur[10]: *i.* continuous and homogeneous breakage of isolated bubbles independently of the drainage flow [8]; *ii.* propagation of a coalescence front as the liquid fraction decreases at the top of the foam [8, 9]; *iii.* avalanches of coalescence for very dry foams below a critical liquid fraction where a film rupture can initiate an abrupt foam collapse due to avalanche of coalescence events over which hundreds of bubbles break in a short time [11, 12].

To control the stability of a foam it is necessary to regulate the coalescence dynamics and the occurrence of these avalanches events. In this work we explore the coupling between the avalanche phenomenon and the drainage flow. To regulate the rate of drainage, we compare a standard non ionic surfactants and an amphiphilic polymer poly(vinyl alcohol), PVA. Foams stabilized by the surfactant present a fast rate of drainage and they quickly become dry over the whole foam height. Foams prepared from the PVA solution drain much more slowly giving a smooth distribution of the liquid fraction with the foam height. We find that avalanches observed for the surfactant foams do not occur in the case of the polymer foams, and we relate this to the difference in liquid fraction profile in the foams. Moreover, we demonstrate that forcing a drainage flow at the top of the foams during the foaming process to control the liquid fraction profile in the PVA and Brij foams enables one to suppress or induce avalanches. As a result, we can recover avalanches in the PVA foams by preparing a homogeneous and dry foam using a low rate of forced drainage during the foaming process. Furthermore, we are able to suppress avalanches in the surfactant foams by preparing homogeneously wet samples, allowing for a more gradual liquid fraction profile to establish in the foams. This work, therefore, demonstrates that the occurrence of avalanches in foams is determined by the liquid fraction profile, which can be

* cecile.monteux@espci.fr

controlled experimentally by tuning the foaming process and the type of amphiphilic molecules used to produce the foams.

EXPERIMENTAL SECTION

Amphiphilic molecules

We use a non-ionic surfactant, BrijO10 purchased from Sigma-Aldrich and an amphiphilic polymer, a partially hydrolyzed poly(vinyl alcohol), PVA, (Mowiol 8-88, M_W = 51 kg/mol from Sigma-Aldrich), containing 88 mol% of vinyl alcohol monomers and 12 mol% of vinylacetate monomers. The concentrations of foaming solutions (20 mM for BrijO10 and 0.1wt% for PVA) are chosen in a way that the amount of surface active elements is the same for both systems, considering the fraction of acetate groups in PVA macromolecules that provide surface activity of the polymer. Since BrijO10 and PVA do not carry any charge we add 20 mM of sodium chloride into all foaming solutions to improve their conductivity response for the experiments on the liquid fraction evolution.

Dynamic surface properties

We measured the dynamic surface tension $\gamma(t)$ using automated tensiometer TRACKER (Teclis-Scientific) in the configuration of rising bubble (see result in ESI). The experiments lasted 5 hours in respect that the dynamics of polymer adsorption is rather slow.

We obtain dilatational surface modulus E by measuring the variation of interfacial tension during oscillation of interfacial bubble area A at a frequency f of 0.1 Hz and a surface deformation amplitude of 3%, with $E = d\gamma \Big/ dA$ with γ the surface tension and A the surface area. The dilatational surface elasticity refers to the real part of the complex modulus $E = E' + iE''$ oscillating the bubble and the dilatational surface viscosity is related to the imaginary part as $\kappa = E'' \Big/ 2\pi f$. The values of E', κ and γ at the 5 hours age of the interface are given in Table I.

Bulk viscosity

We measured viscosity of foaming solution using a AR-G2 Rheometer (TA Instruments) in a cone-plate geometry with the cone angle 2°, diameter 40 mm, truncation 52 mm. We performed frequency sweeps in the range of 5-1000 Hz to ensure the Newtonian behaviour of the foaming solutions.

All measurements are made at 25 °C, and with a solvent trap to avoid evaporation. The viscosity data are presented in Table I.

TABLE I. Stabilizer type, surface tension γ, the surface dilatational elasticity E' and viscosity κ measured by the oscillating bubble method at a frequency of $f = 0.1Hz$ and a surface deformation amplitude of 3%, and bulk viscosity η for the foaming solutions used in the experiments.

Stabilizer	γ, mN/m	E', mN/m	κ, mN·s/m	η, mPa·s
PVA	49.1	10.1	5.1	1.1
BrijO10	31.3	1.2	7.0	1.4

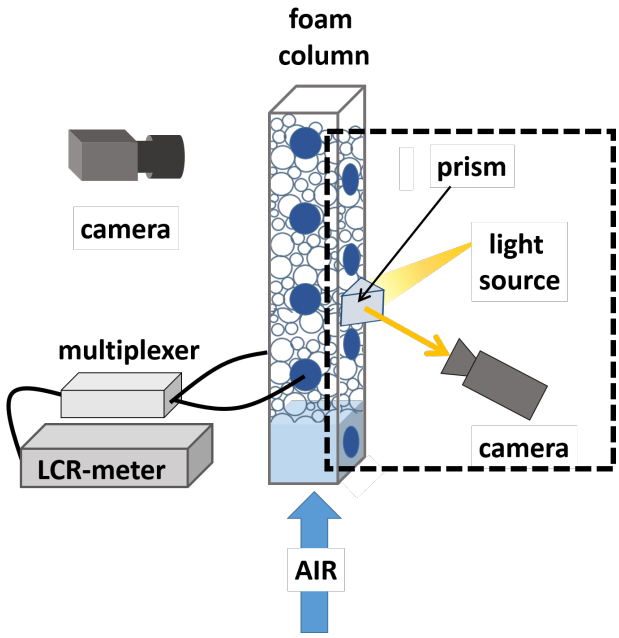

FIG. 1. Experimental setup: a plexiglass cell has 8 pairs of electrodes, the first one is covered by the foaming solution, each pair of electrodes is connected to the LCR-meter equipped by a multiplexer, a camera takes picture to follow the evolution of the foam height. Dashed zone: imaging of the bubbles at the cell surface is due to camera which takes pictures through a prism.

Foaming process

To create the foams, air is forced through a porous frit that is localized at the bottom of an acrylic cell (250 mm height, 30 mm x 30 mm square cross section) covered by 50 ml of solution. During the experiment the acrylic cell is sealed on the top to avoid evaporation.

The initial bubble radius R_b^{init} is controlled by the size of the pores and most of the experiments are performed with R_b^{init} = 75 μm. We measure R_b^{init} straight after their formation by imaging a thin layer of foam using a microscope [13].

The foaming process lasts until the bubbles fill the cell from bottom to top. We take this moment as a zero age of a studied foam. As it takes several minutes to fill the column with foam, the continuous phase starts draining through the foam already during the foaming process. As a consequence, the initial liquid fraction profile right

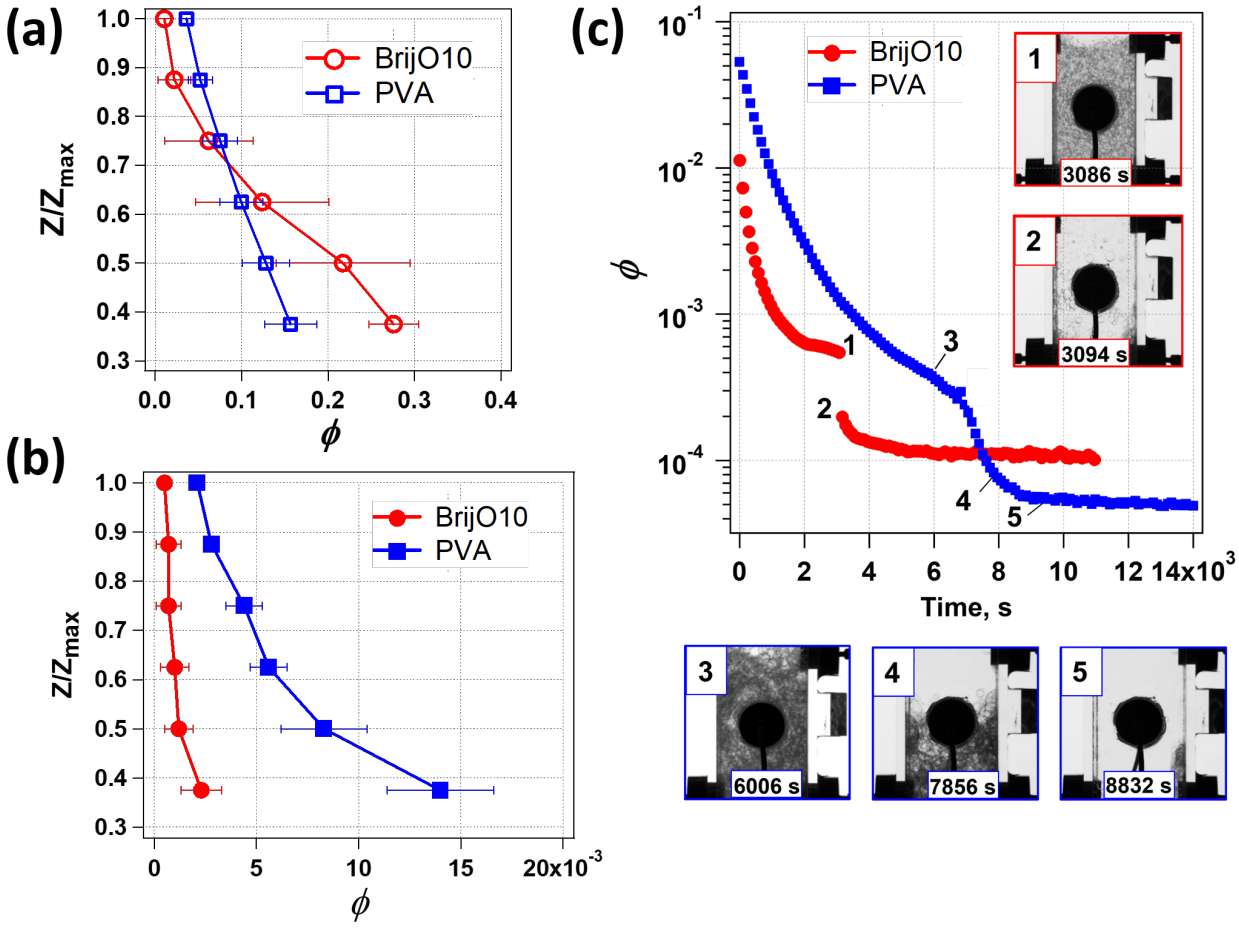

FIG. 2. Distribution of the liquid fraction along the normalized foam height in of a foam stabilized by 20 mM of Brij O10 (red circles) and of a foam stabilized by 0.1wt% of PVA (blue squares) at (a) the initial stage of foam life-time (empty symbols) and (b) before occurrence of coalescence avalanches (filled symbols). Lines are guides for the eye. (c) Evolution of the liquid fraction at a given pair of electrodes ($Z/Z_{max} = 0.875$) for a foam stabilized by 20 mM of BrijO10 (red circles) and of a foam stabilized by 0.1wt% of PVA (blue squares). Numbered photos illustrate the corresponding points at the curves. The error bars on the liquid fraction profiles are determined by analysing three independent experiments.

after the foaming process may not be homogeneous over the foam height, the top of the foam being drier than the bottom.

Foaming process proceeding with a forced drainage flow

To obtain foams with a homogeneous liquid fraction profile at zero age, we conduct a series of experiments where the foaming solution continuously circulates through the sample during the foaming process. For this purpose we use a syringe pump to inject the surfactant or the polymer solution at the top of the foam and evacuate the drained liquid at the bottom of the foam column. The rate of the forced drainage flow enables us to control the initial liquid fraction. For a flow rate Q of Q=0.1 ml/min we obtain an initial liquid fraction ϕ_i=0.02 and for Q=20 ml/min we obtain a liquid fraction ϕ_i=0.1. When the column is filled with the foam, the forced drainage flow is stopped and the foam is left to drain spontaneously under the action of gravity.

Measurement of liquid fraction evolution

We obtain ϕ values from the foam electrical conductivity [14] measured by pairs of circular electrodes which have the radius of 4 mm and located at various positions along the cell height. The electrodes are connected to an impedance meter (LCR Meter, Chroma 11021) operating at a frequency of 1kHz and at voltage 1V. The apparatus measures the resistance of a parallel resistor–capacitor equivalent circuit, the value which is reciprocal to conductivity. Simultaneously we observe the foam height using a camera. The setup is sketched in Figure 1. For all the liquid fraction profiles, the ϕ values corresponding to one given electrodes are the averages obtained for

three independent experiments. The critical liquid fractions ϕ^* are determined by averaging the values obtained from five electrodes in each of these three experiments.

Foam imaging at the wall of the column

During the ageing of the foam we take pictures of the bubbles at the surface of the measuring cell trough a prism attached to the cell wall (see the dashed zone in Figure 1). Using an open source image processing program ImageJ, we determine surface area A_b of bubbles and we convert it into the bubble radii $R_{b,surf} = \sqrt{A_b/\pi}$. The value $R_{b,surf}(0)$ corresponds to the zero time. The Sauter mean radius $\langle R_{b,surf}\rangle = \sum_{i=1}^{n} n_i R_{b,surf}^3 / \sum_{i=1}^{n} n_i R_{b,surf}^2$ averaged over n bubbles at the image increases during the foam ageing. Since the size of the analyzed image is restricted by the perimeter of the prism, n decreases with time. We perform the analysis until the number of bubbles becomes less than 100.

RESULTS AND DISCUSSION

We compare the ageing of foams stabilized either with a non-ionic surfactant BrijO10 or with an amphiphilic polymer, a partially hydrolyzed PVA which presents a slow rate of drainage [15].

The foaming process lasts several minutes and hence proceeds simultaneously with the spontaneous gravity-induced drainage of the continuous phase in the created foam column. Therefore we observe a gradient of the liquid fraction along the foam height at early times in the experiment [16] (Figure 2a). Surfactant-stabilized foam has a steep profile of ϕ with a very dry foam on the top and most of the liquid collected on the bottom of the cell. Reduced drainage in PVA-stabilized foam results in a wetter foam at the top, which liquid fraction increases smoothly as the height decreases.

At longer times, the liquid fraction continuously decreases due to drainage without any change in the foam height. In Figure 2b we show the liquid profile distributions that correspond to the last moment before BrijO10-stabilized foam collapses and for the PVA foam of the same age. For BrijO10, an almost vertical $\phi(z)$ profile develops along the foam height z during the foam ageing. When the liquid fraction approaches ϕ^*=0.0006 ± 0.0003 an avalanche proceeds and thousands of bubbles break simultaneously. The surface of electrodes is no more covered by the foam and the registered signal abruptly drops at a given height as shown in Figure 2c.

In the case of the polymer-stabilized foam coalescence proceeds in a more gradual manner over a total duration of 2000 seconds, as bubbles burst layer by layer, starting from the top of the column (Figure 2c). A coalescence front propagates and the foam collapse is obtained. As the foam front reaches the position of an electrode, its surface becomes covered by the foam only partially reducing the measured value. As a result, the time-dependency of the liquid fraction represents a continuous decrease with a change in the curve slope that occurs at the moment of the foam front arrival and hence there is no intermittence in the liquid fraction evolution, as we show in Figure 2c. The plateau values measured at the late stages of both experiments is due to conductivity of the wetting films at the surface of the cell.

The existence of a critical value ϕ^* for the liquid fraction at which the foam collapses by coalescence avalanches was previously reported by other authors [17–19]. Carrier and Colin [17] observed similar behaviour for foams stabilized by common surfactants and their critical values of ϕ^* are in agreement with our data. Despite the fact that the origin of ϕ^* is still under debate, it was demonstrated that its value almost saturates at high concentrations above *cmc* and that it is independent of the bubble size and the initial liquid fraction of the foam except for small bubbles [9] which value of ϕ^* is two orders of magnitude higher than in common foams. The value of ϕ^* can be affected by the bulk and surface shear viscosity of the foaming solution as well as interfacial tension [18, 20], therefore, we make sure that these parameters are approximately the same for our two experimental systems (see Table I). From the model of Biance et al. [18] we estimate the decrease of ϕ^* for about only 2 times explaining why the critical liquid fractions are very close for both systems but not why the coalescence process is much more catastrophic for the BrijO10 than for the PVA.

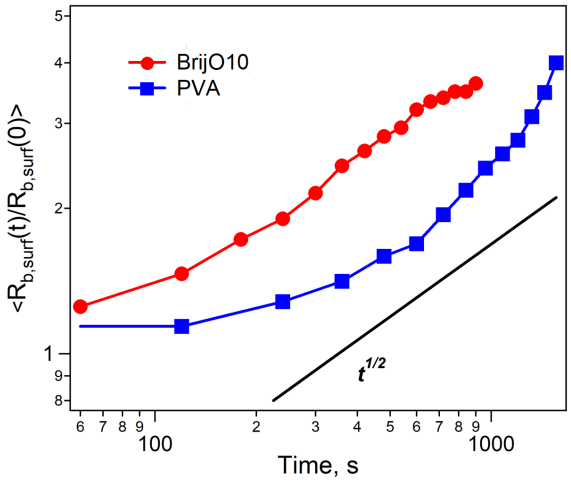

FIG. 3. Relative increase of the average bubble radius measured at the surface of the measuring cell for the foam stabilized by BrijO10 (red circles) and PVA (blue squares) with $R_b^{init} = 75\mu m$. The black solid line has the slope of $t^{1/2}$, where t is time. Lines are guides for the eyes. The error bars depend on the threshold which is used to transform the image into a binary one and they are within the size of the used symbols.

Even though we do not observe coalescence avalanches

in PVA-stabilized foams in spontaneous drainage experiments, we observe single bubble coalescence events in the middle of the foam column. We reveal their occurrence with the analysis of the average bubble size evolution from the images taken at the surface of the cell. The corresponding curves are shown in Figure 3. The presented values $\langle R_{b,surf} \rangle$ do not correspond directly to the size of the bubbles in the bulk of the foam [21], but they give an idea on the rate of the bubble size evolution [22]. In the case of BrijO10, we observe an induction period which is determined by the initial polydispersity of bubble size [3]. Afterwards the average radius $\langle R_{b,surf}^{BrijO10} \rangle$ increases linearly with the square root of the foam age, which is characteristic for the coarsening of dry foams [23–25]. In the case of the PVA-stabilized foams $\langle R_{b,surf}^{PVA} \rangle$ presents a faster increase which can only be explained by individual bubble coalescence in addition to the coarsening. These individual coalescence events, however, have no crucial influence on the foam height: they do not initiate a collective film rupture in the bulk of the foam and the main coalescence front still propagates from the top to the bottom of the foam column. Understanding of the mechanism at play in coalescence phenomena is beyond the scope of the article. However this result demonstrates that the increase of the bubble surface area caused by coalescence in PVA foams does not increase the probability of rupture in contrary to other studies of the literature [12, 26].

We assume that the reason of the difference in the avalanches phenomena in the two foams originates from the difference in the liquid fraction profiles that are developed in the foams under drainage of different rate. As shown in Figure 2b fast drainage in the BrijO10 case leads to the development of an almost vertical ϕ profile during the foam ageing. The main part of the curve lays in the region of ϕ^* that sets the limit of the foam stability. Therefore, in the next moment the avalanches affect a considerable fraction of the foam volume leading to an abrupt drop of the foam height. At the same age, the foam stabilized by PVA is much wetter at the level of each electrode and the liquid distribution is more gradual due to the reduced drainage. Apparently, the size of electrodes does not allow to resolve the liquid profile on the very top of the foam column where we expect to have the largest gradient of the liquid fraction with height. We speculate that in this case the portion of the foam that is under critical condition corresponds roughly to a layer of bubbles, which burst gradually leading to a slow decrease of the foam height. Therefore, the foam vanishing is less catastrophic.

To verify our assumption, we prepare foams with a homogeneous liquid fraction profile by forcing the continuous phase to flow through the foam during the foaming process and evacuating it at the bottom of the foam with the same flow rate. Controlling the flow rate of the forced drainage flow enables us to control the initial liquid fraction of the foams. We then stop the forced drainage and let the foam age on its own. As we show in Figure 4a, we prepare a dry PVA foam with a steep initial liquid fraction profile with a liquid fraction equal to 0.02 close to the liquid profile of the BrijO10 foam in Figure 2a. As drainage proceeds, the liquid fraction decreases in the same manner over the foam height and the liquid fraction profile remains steep over time. When the liquid fraction reaches 0.0007 ± 0.0005 , we observe an avalanche of coalescence that gives a drop in $\phi(t)$-dependence shown in Figure 4c. Foam collapse in this case repeats the scenario of a BrijO10 foam: the liquid fraction initially decreases due to natural drainage and when ϕ^* is approached it abruptly drops because of avalanches of coalescence events. Thus, we demonstrate that the occurrence of the coalescence avalanches is primarily governed by the liquid fraction profile in the foam. To ensure that PVA foam collapses under the same critical condition regardless the bubble size, we perform the same forced drainage experiment with a different initial bubble radius, $R_b^{init} = 100$ μm. The critical liquid fraction is the same as for both formerly studied foams indicating its indifference to the bubble size (see ESI). This is in line with experimental results obtained with surfactants [17–19], the same, however, had never been proven for polymer-stabilized foams.

After showing that avalanches in the PVA foams can be triggered by preparing a foam with a steep and low liquid fraction profile, the next question is to know whether we can prevent avalanches for the surfactant-stabilized foams by preparing BrijO10 foams with a smooth liquid fraction profile. Using the forced drainage set up, we prepare a wet BrijO10 foam with an initial liquid fraction equal to 0.1 (Figure 4a). Over time, the liquid fraction profile smoothens (Figure 4b) and resembles the one for the PVA foam in the experiment with the free drainage. In this case, the kinetic dependency of the liquid fraction evolution for a given electrode do not have any rupture and we do not observe any avalanche (Figure 4c). Indeed, in the BrijO10 foam prepared in such manner a coalescence front propagates as it was observed previously in Figure 2c for PVA foams.

To summarize, our results show that the liquid fraction profile in the foams, which is controled by the rate of drainage determines whether foam coalescence will occur in catastrophic avalanches or through a coalescence front propagating from the top to the bottom of the foams. This behaviour can be tuned either by the type of amphiphilic stabilizer or by the foam preparation method. The difference in these two extreme situations lies in the propagation velocity of the coalescence front. We report in Figure 5 the rate of the coalescence propagation front as a function of a gradient of the liquid fraction profile along the foam height, $\Delta\phi/(\Delta Z/Z_{max})$. The highest propagation rates of the order of $5.10^{-3} m.s^{-1}$ correspond to centimetric avalanches propagating in a few seconds and they are observed at low values of liquid fraction gradients obtained either for BrijO10 foams using the standard foaming method or for the PVA foams using the forced drainage for the foam preparation with ϕ_i=0.02.

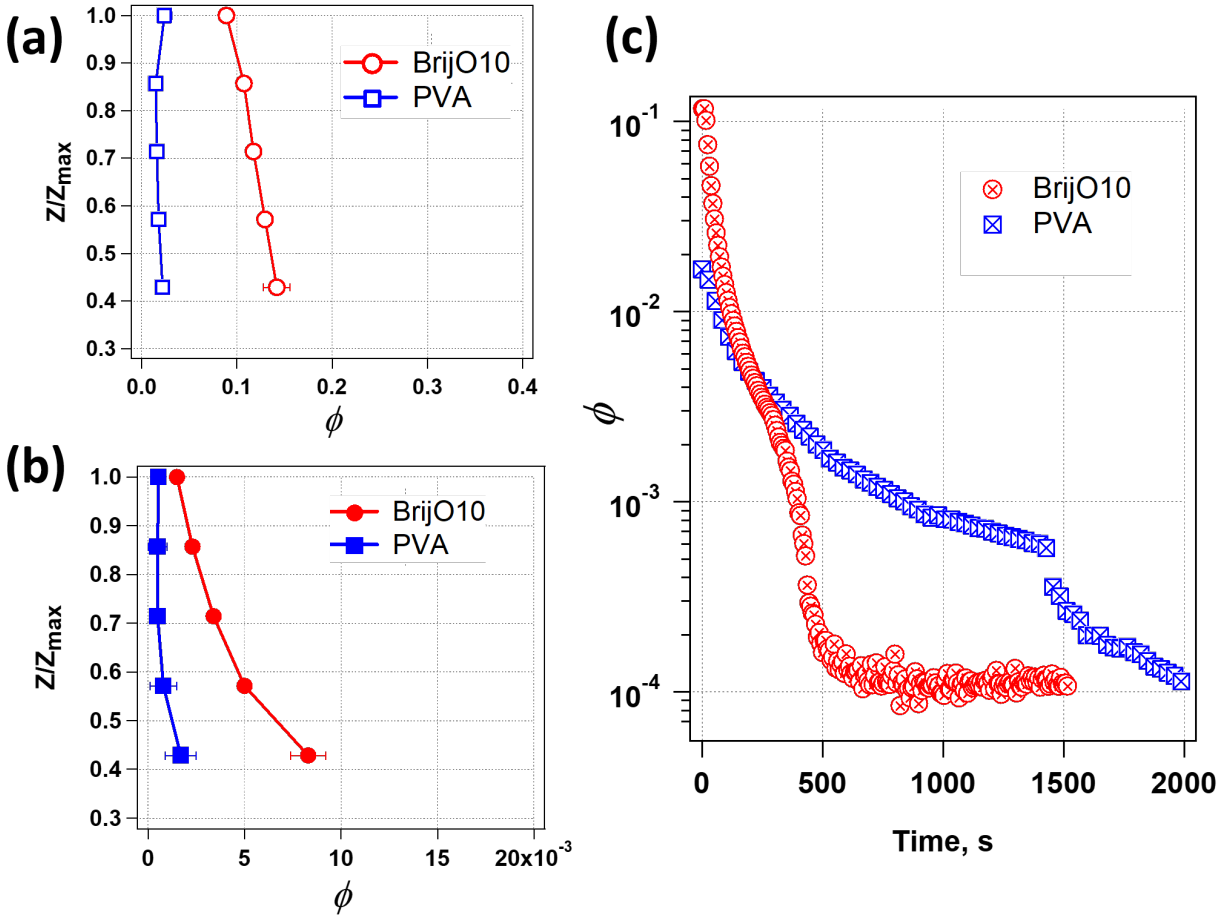

FIG. 4. Distribution of the liquid fraction along the normalized foam height in of a foam stabilized by 20 mM of Brij O10 prepared with the forced drainage at the flow rate 20 ml/min (red circles) and of a foam stabilized by 0.1wt% of PVA prepared with the forced drainage at the flow rate 0.1 ml/min (blue squares) at (a) the initial stage of foam life-time (empty symbols) and (b) before occurrence of coalescence avalanches (filled symbols). Lines are guides for the eye. (c) Evolution of the liquid fraction at a given pair of electrodes ($Z/Z_{max} = 0.7$) for a foam stabilized by 20 mM of BrijO10 (red crossed circles) and of a foam stabilized by 0.1wt% of PVA (blue crossed squares).

Lower propagation rates of the order of $10^{-5} m.s^{-1}$ are observed for larger values of $\Delta\phi/(\Delta Z/Z_{max})$ and they correspond to a slow decrease of the foam height for PVA foams obtained with the simple foaming method. Interestingly for larger values of $\Delta\phi/(\Delta Z/Z_{max})$, the coalescence rate increases up to $10^{-4} m.s^{-1}$. These data points corresponds to the experiments made with the BrijO10 foams prepared with forced drainage and starting at ϕ_i=0.1. In this latter case, the faster propagation of the coalescence front is due to the fast drainage of the BrijO10 foams, which causes the top of the foams to dry more quickly.

CONCLUSIONS

By comparing foams stabilized either by a surfactant or a surface active polymer, in which coalescence occurs under similar critical conditions but which differ by the drainage flow, we show that the foam collapse is governed by the distribution of the liquid fraction over the foam height. In the case of the surfactant foams, the liquid fraction profile is steep and the foam is homogeneously dry. When ϕ^* is approached a collective rupture of bubbles in large avalanches proceeds. For the polymer-stabilized foams, where the liquid fraction profile evolves more gradually with the foam height, the avalanches are suppressed and a coalescence front slowly propagates from the top to the bottom of the foam. Moreover, we demonstrate that one can induce or suppress avalanches by controlling the liquid fraction distribution while forcing a drainage flow at the top of the foam during the foaming process. As a result, we can recover avalanches in the PVA foams by preparing a homogeneous and dry foam using a low rate of forced drainage during the foaming process. Moreover we are able to suppress avalanches in the surfactant foams by preparing initially wet samples, for which a more gradual liquid fraction profile es-

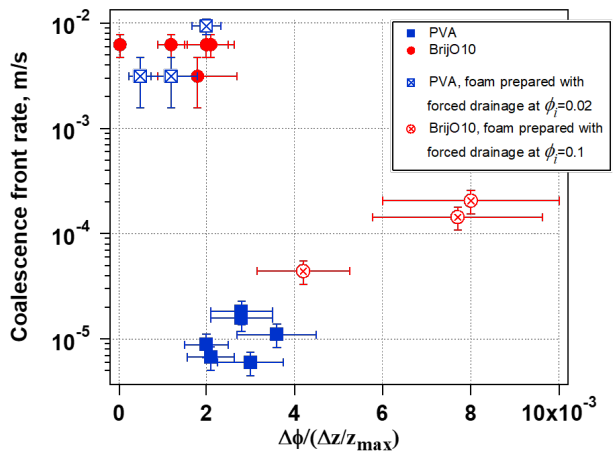

FIG. 5. Relation between the gradient of the liquid fraction distribution along the foam height and the occurrence of coalescence avalanches in BrijO10- (red circles) and PVA-stabilized (blue squares) foams: full symbols are for the experiments for foams prepared by simple foaming, empty crossed symbols are for foams prepared with the forced drainage.

tablishes in the foams. Finally we show that the velocity of the coalescence propagation front is controlled by the liquid fraction profile in the foams. In conclusion, our study demonstrates the strong coupling between drainage and coalescence and provides guidelines to control and suppress avalanches phenomena by varying the type of stabilizer used and the foaming process.

CONFLICTS OF INTEREST

There are no conflicts to declare.

ACKNOWLEDGEMENTS

We acknowledge the technical support of Jérémie Sanchez, Vincent Klein, Ludovic Olanier and Alexandre Lantheaume and fruitful discussions with Nadège Pantoustier and Patrick Perrin. This work was financially supported by ANR FOAMEX grant number ANR-17-CE08-0016.

[1] P. Stevenson, *Foam engineering: fundamentals and applications* (John Wiley & Sons, 2012).
[2] C. Hill and J. Eastoe, Foams: From nature to industry, Advances in Colloid and Interface Science **247**, 496 (2017).
[3] I. Cantat, S. Cohen-Addad, F. Elias, F. Graner, R. Höhler, O. Pitois, F. Rouyer, and A. Saint-Jalmes, *Foams: Structure and Dynamics* (Oxford University Press, 2013).
[4] S. Hutzler and D. Weaire, Foam coarsening under forced drainage, Philosophical magazine letters **80**, 419 (2000).
[5] S. Hilgenfeldt, S. A. Koehler, and H. A. Stone, Dynamics of coarsening foams: accelerated and self-limiting drainage, Physical review letters **86**, 4704 (2001).
[6] A. Saint-Jalmes and D. Langevin, Time evolution of aqueous foams: drainage and coarsening, Journal of Physics: Condensed Matter **14**, 9397 (2002).
[7] A. Saint-Jalmes, Physical chemistry in foam drainage and coarsening, Soft Matter **2**, 836 (2006).
[8] D. Monin, A. Espert, and A. Colin, A new analysis of foam coalescence: from isolated films to three-dimensional foams, Langmuir **16**, 3873 (2000).
[9] Z. Briceño-Ahumada, W. Drenckhan, and D. Langevin, Coalescence in Draining Foams Made of Very Small Bubbles, Physical Review Letters **116**, 1 (2016).
[10] E. Rio and A.-L. Biance, Thermodynamic and mechanical timescales involved in foam film rupture and liquid foam coalescence, ChemPhysChem **15**, 3692 (2014).
[11] W. Müller and J. Di Meglio, Avalanches in draining foams, Journal of Physics: Condensed Matter **11**, L209 (1999).
[12] N. Vandewalle, H. Caps, and S. Dorbolo, Cascades of popping bubbles, Physica A: Statistical Mechanics and its Applications **314**, 320 (2002).
[13] T. Gaillard, C. Honorez, M. Jumeau, F. Elias, and W. Drenckhan, A simple technique for the automation of bubble size measurements, Colloids and Surfaces A: Physicochemical and Engineering Aspects **473**, 68 (2015).
[14] K. Feitosa, S. Marze, A. Saint-Jalmes, and D. J. Durian, Electrical conductivity of dispersions: From dry foams to dilute suspensions, Journal of Physics Condensed Matter **17**, 6301 (2005), 0507381.
[15] R. Deleurence, T. Saison, F. Lequeux, and C. Monteux, Time scales for drainage and imbibition in gellified foams: Application to decontamination processes, Soft Matter **11**, 7032 (2015).
[16] P. Yazhgur, E. Rio, F. Rouyer, F. Pigeonneau, and A. Salonen, Drainage in a rising foam, Soft matter **12**, 905 (2016).
[17] V. Carrier and A. Colin, Coalescence in draining foams, Langmuir **19**, 4535 (2003).
[18] A. L. Biance, A. Delbos, and O. Pitois, How topological rearrangements and liquid fraction control liquid foam stability, Physical Review Letters **106**, 1 (2011).
[19] E. Carey and C. Stubenrauch, Foaming properties of mixtures of a non-ionic (C12DMPO) and an ionic surfactant (C12TAB), Journal of Colloid and Interface Science **346**, 414 (2010).
[20] A. L. Biance, S. Cohen-Addad, and R. Höhler, Topological transition dynamics in a strained bubble cluster, Soft Matter **5**, 4672 (2009).
[21] Y. Wang and S. J. Neethling, The relationship between the surface and internal structure of dry foam, Colloids and Surfaces A: Physicochemical and Engineering Aspects **339**, 73 (2009).
[22] A. E. Roth, B. G. Chen, and D. J. Durian, Structure and coarsening at the surface of a dry three-dimensional aqueous foam, Physical Review E - Statistical, Nonlinear,

and Soft Matter Physics **88**, 1 (2013).
[23] D. Durian, D. Weitz, and D. Pine, Multiple light-scattering probes of foam structure and dynamics, Science **252**, 686 (1991).
[24] J. A. Glazier and D. Weaire, The kinetics of cellular patterns, Journal of Physics: Condensed Matter **4**, 1867 (1992).
[25] N. Isert, G. Maret, and C. M. Aegerter, Coarsening dynamics of three-dimensional levitated foams: From wet to dry, The European Physical Journal E **36**, 116 (2013).
[26] E. Forel, B. Dollet, D. Langevin, and E. Rio, Coalescence in two-dimensional foams: A purely statistical process dependent on film area, Physical review letters **122**, 088002 (2019).